APPENDIX AVAILABLE ON THE HEI WEB SITE

Research Report 178

National Particle Component Toxicity (NPACT) Initiative Report on Cardiovascular Effects

Sverre Vedal et al.

Section 1: NPACT Epidemiologic Study of Components of Fine Particulate Matter and Cardiovascular Disease in the MESA and WHI-OS Cohorts

Appendix E. Oxidative Potential

Note: Appendices that are available only on the Web have been assigned letter identifiers that differ from the lettering in the original Investigators' Report. HEI has not changed the content of these documents, only their identifiers.

Appendix E was originally Appendix D

Correspondence may be addressed to Dr. Sverre Vedal, University of Washington, Department of Environmental and Occupational Health Sciences, Box 354695, 4225 Roosevelt Way NE, Suite 100, Seattle, WA 98105-6099; email: *svedal@uw.edu*.

Although this document was produced with partial funding by the United States Environmental Protection Agency under Assistance Award CR–83234701 to the Health Effects Institute, it has not been subjected to the Agency's peer and administrative review and therefore may not necessarily reflect the views of the Agency, and no official endorsement by it should be inferred. For the research funded under the National Particle Component Toxicity initiative, HEI received additional funds from the American Forest & Paper Association, American Iron and Steel Institute, American Petroleum Institute, ExxonMobil, and Public Service Electric and Gas. The contents of this document also have not been reviewed by private party institutions, including those that support the Health Effects Institute; therefore, it may not reflect the views or policies of these parties, and no endorsement by them should be inferred.

This document was reviewed by the HEI NPACT Review Panel but did not undergo the HEI scientific editing and production process.

APPENDIX D: Oxidative Potential

- **QC data for DTT measurements**
- **Comparison of DTT reactivity in integrated PM samples with collection periods of 1-14 days**

There is increasing scientific support for theories proposing that oxidative and nitrosative stress represent a primary pathway leading to the respiratory and systemic inflammatory responses associated with PM exposure (Li 2002; Xia 2004). The capacity of PM to elicit oxidative stress reflects both the oxidant-generating properties of particles and their ability to stimulate cellular generation of reactive oxidant species. From a mechanistic point of view, it is appealing to use biologically relevant properties of PM to characterize "exposure" in epidemiologic studies, rather than imperfect surrogates such as the total mass concentration, or even concentrations of various components. One of the most widely described approaches to measure the oxidative potential of PM samples is to measure di-thiothreitol (DTT) reactivity (Kumagai 2002; Li 2003).

Here we describe work on measuring DTT from MESA Air/NPACT monitoring filters and developing models to predict DTT based on the PM2.5 component data. We have not attempted to predict DTT for each PM speciation sample obtained in the MESA Air/NPACT campaign with an eye to developing a prediction model for oxidative potential and then predictions for MESA Air study participants that might be used subsequently in health effects analyses. In light of the relatively poor predictive ability of our PM component models in NPACT, models based on measured data, we felt that similar models based on predicted values would produce even more uncertain predictions.

Sample selection

Measurements of DTT reactivity were conducted on 314 extracts of PM samples from quartz filters that were collected in each of the six MESA Air/NPACT metropolitan regions. Selection of the filters was first divided between summer and winter seasons and included each

of the twenty-six fixed sites in the MESA Air study. For each site, an average of six samples was selected during each season. To the extent possible, samples selected from all sites within a city were concurrent. However, quartz filter samples which had two aliquot punches removed for replicate analysis for OC, EC and those classified as invalid due to flow rate or sample duration errors were excluded from the analysis set. This prevented assembling complete sets of concurrent samples for each city due to the random occurrence of both replicate analyses and invalid samples.

Sum of parts study. Thirty-six filters were extracted and analyzed using the DTT microplate assay for a "sum of parts" study. The objective was to evaluate whether sampling with a single filter for an extended period of time would provide comparable results to the summation of values obtained from multiple filters used for shorter durations, but having the same combined sampling time. Three, two-week sampling sessions were conducted in Los Angeles, CA (6/1/09-6/15/09, 6/15/09-6/29/09, and 6/29/09-7/13/09). For each session, a single two week sample was collected along with four intermediate samples (3-4 days) covering the same time period. Additionally, with each session, eight daily filters were collected corresponding to two of the intermediate filters.

Filters were collocated on a roof top of a University of Southern California building. After sampling, filters were placed in individual plastic petri dishes with lids, wrapped in aluminum foil, sealed in ziplock bags and stored in a -20°C freezer until analyzed. These samples have been extracted and DTT reactivity measured. Description and interpretation of data from these samples is reported in Appendix D.

Laboratory analysis

DTT assay: The dithiothreitol (DTT) assay measures the presence or formation of reactive oxygen species via formation of the DTT-disulfide (Li 2002). Unreacted DTT is detected colorimetrically after reaction with 5,5'-dithiobis-(2-nitrobenzoic acid) (DTNB), producing 5-mercapto-2-nitrobenzoic acid. The rate of disappearance of DTT is proportional to the oxidant activity. The assay uses 1,8-phenanthraquinone as a positive control and the absence of added oxidant species as a negative control (Kumagai 2002).

We adapted the procedure of Li et al (Li 2003) for use with a microplate reader in order to improve sample throughput, sensitivity and precision. PM samples on quartz filters are extracted by ultrasonication in methanol (7 mL) for 60 minutes. The extract is concentrated to 1 mL under a flow of nitrogen at 50°C in a Turbovap evaporative concentrator and then filtered through a 0.2 μm PTFE syringe filter. The extract is reduced to dryness and reconstituted in 65 μL of methanol. After vortexing, water and phosphate buffer are also added to the sample. To measure DTT reactivity, the entire extract is then incubated in the presence of DTT in a 96 well plate. At designated time points (0, 10, 20, 30, 40, 50 minutes) aliquots of the reaction mixture are withdrawn and added to microplate wells containing tris HCl in 20 mM EDTA and DTNB (5,5'-dithiobis-(2-nitrobenzoic acid)). Absorption at 412 nm is recorded. The rate of DTT consumption is calculated from a plot of absorbance vs. time, and this value is corrected for atmospheric oxidation of DTT calculated from a blank filter extract time series.

Quality Control:

Data quality was monitored using control charts for the phenanthraquinone (PQ; positive control), filter blank (blank filters extracted with each batch of filters), and reagent blanks (one column of the 96 well plate that contains buffer, water, methanol, and DTNB, but no DTT).

Control charts for the PQ and reagent blanks are included in Appendix D2.

The limit of quantification (LOQ) was set equal to the average DTT reactivity of the blank filter + 2 std deviations (0.995 μM/min). Overall summary statistics for the DTT reactivity measurements are listed in Appendix Table D.1.

We used quartz filters for the DTT analysis, as these were the only filters available to use for this assay. We recognize that DTT reactivity as measured for particles collected on quartz filters may well differ from reactivity of the same particles collected on Teflon filters. The quartz fibers themselves are unlikely to contribute directly to the DTT reactivity because DTT reactivity is measured on a solvent extract of the particles, which is filtered through a 0.25 micron syringe filter before undergoing the reaction with DTT. However, semivolatile material adsorbed onto the quartz filter would contribute to the particle extract and could potentially provide a small contribution to the measurements of DTT reactivity. Nevertheless, we do not believe that potential differences in DTT reactivity due to the choice of sample collection media adversely affect the primary goals of our study.

Furthermore, it is worth emphasizing that the DTT assay is not standardized across laboratories. Thus the absolute values of the DTT reactivity differ between laboratories based on each laboratory's choice of sampling media, extraction solvent and reagent concentrations and reaction conditions for the actual measurement of DTT reactivity. Thus, it is not appropriate to compare absolute values of DTT reactivity between laboratories. However, it is reasonable to expect that relative measures of DTT reactivity are similar between laboratories: samples that exhibit high levels of DTT reactivity using one laboratory's procedures should also be highly reactive by another laboratory's procedure.

Statistical methods

The primary goals of the statistical analysis are to: (1) evaluate trends in DTT reactivity across locations and seasons, and (2) to use multivariate statistical methods to identify chemical components of $PM_{2.5}$ that are predictive of DTT reactivity in the data set.

Following a brief exploratory analysis of the response (DTT reactivity) and the predictors to inform modeling choices, the general stages of variable selection and model building are as follows:

1. Identify plausible predictors of the response by use of the LASSO and best subsets regression *without* $PM_{2.5}$. $PM_{2.5}$ has many specific chemical components – the predictors – and ideally these explain DTT reactivity better than the aggregate. (Note, however, that the numerical values of $PM_{2.5}$ concentration are not a strict aggregate of the other predictors: the sum of the predictor concentrations does not equal $PM_{2.5}$ concentration.)
2. Upon selecting variables, add $PM_{2.5}$ concentration to the regression model to assess its significance and predictive value. Its addition may have implications for the significance of other variables.
3. Last, add fixed effects for location, season, and the interaction between them to the model to assess whether they are significantly predictive of DTT reactivity *after* controlling for $PM_{2.5}$ and its chemical components.

Exploratory description of DTT reactivity and predictors

Response and predictors: normalization and data cleaning

All of the predictors are expressed as concentrations in units $\mu g/m^3$, that is, normalized by the air volume passing through the filters. DTT reactivity is measured as a rate in ng/min, absorbance vs. time. As these scales are not comparable we also normalize the DTT reactivity, the response, by the calculated air volume, resulting in units of $ng/min/m^3$.

Another option, explored but not pursued in this treatment, is to further normalize the response and the predictors by the $PM_{2.5}$ concentration, which essentially turns the predictors into "mass fractions": fractions of $PM_{2.5}$.

There were 274 observations of the response and predictors. The removal of partially missing data reduced this to 248 observations. Two observations had 0 recorded for the quartz filter air flow, making normalization of the response impossible; this reduced the observations to 246. Last, one observation was removed due to an apparent extreme value (outlier) in one of the components. The final data set contained 245 observations.

Data description: figures and tables

Appendix Figure D.1 illustrates the distribution of the DTT reactivity with a frequency histogram, with summary statistics shown in Appendix Table D.2. The variable is contained in the rough range of 0 to 30 $ng/min/m^3$, with no heavy tails; thus, it is reasonable to attempt to fit models for the response without additional transformation.

Appendix Figure D.2 gives evidence of seasonal variation by location. The locations of the observations are Baltimore, Chicago, Los Angeles, Los Angeles-Coastal, Los Angeles-Riverside, New York, New York-Rockdale, St. Paul, and Winston-Salem; the seasons are rough categorization of Summer or Winter. The number of observations that contributed to each boxplot are included in the x-axis for each location.

Generally, DTT reactivity appears to be higher in Winter; most noticeably in Los Angeles, St. Paul, and Winston Salem. New York and New York-Rockdale appear to demonstrate the opposite behavior, with DTT reactivity apparently lower from samples taken in Winter from these locations than is Summer, though this is not conclusive. With many of these, the low numbers of observations should give one pause before interpreting too strongly. Several of these location-seasons have very small numbers of observations, Los Angeles-Riverside in Winter being the most extreme with only 1 observation.

The 52 predictors including $PM_{2.5}$ are numerically summarized in Appendix Table D.3. Before calculating the summaries, each of the predictors was checked against its recorded limit of detection; if lower than the limit of detection, the limit of the detection was inserted in place of the original value. The number of observations for which this occurred is recorded for each predictor.

While the original scale of these predictors is in units of $\mu g/m^3$, due to some of the low concentrations, the table is summarized in units of ng/m^3, or $1000 \times \mu g/m^3$. Notably large mean concentrations besides $PM_{2.5}$ are the different carbons lac (light absorbing carbon), EC (elemental carbon), and OC (organic carbon), and S (Sulfur).

There are several predictors with substantial numbers of observations less than their limit of detection. The most extreme case by far is W, with only 11 values *above* the limit of detection. Hence, W is omitted from the analysis due to the dearth of useful data.

Correlations between predictors

Variable selection and regression in general is complicated by the existence of highly correlated variables, with no firm rules on how to treat such correlations. For groups of

correlated variables, simple solutions range from using one as a proxy to averaging their standardized values to doing nothing. We adopted various treatments for correlated variables.

Rather than show all pairwise correlations, we identify loosely defined groups for which at least one pairwise correlation is above 0.65. In Appendix Table D.5 the elements are assigned to (mutually exclusive) groups, with "groups" 4 and 5 consisting of single elements.

For Group 1, each pair within the four predictors (Ba, Cu, K, Sr) are highly correlated. As they are all similar elements, mostly alkali metals, we take the average of the four predictors as a representative for all of the four.

For Group 2, as Si is highly correlated with Al, we use the value of Al to represent most of the information of the Si term.

For Group 3 we use EC to represent Fe and light absorption coefficient (LAC). We note that EC has the highest correlation of the three with the response.

Groups 4 and 5 each contain a single pair of correlated components. We chose to retain both Na and V of Group 4 as candidate predictors. However, the correlation of S and P is about 0.8, so we created a new variable based on their standardized values, "Group B".

After dealing with the high correlation issues, the number of predictors is reduced from 51 to 44. There is some subjectivity in such choices, which should be remembered in interpreting the subsequent models.

Variable selection

The purpose of this analysis is to select a group of predictors jointly predictive of DTT reactivity. There are 245 observations and 43 variables to choose from. The large number of

predictors and comparatively few observations make the model selection problem crucial. We review two general methods of selection and compare the results.

LASSO

The LASSO refers to the **L**east **A**bsolute **S**hrinkage and **S**election **O**perator. Consider the following linear regression model with standardized predictors:

$$Y_i = \beta_0 + \beta_1 x_{1i} + \beta_2 x_{2i} + \ldots + \beta_p x_{pi} + \varepsilon_i = \beta_0 + \mathbf{x}_i^T \boldsymbol{\beta} + \varepsilon_i \qquad \text{eqn. (1)}$$

The coefficients $\boldsymbol{\beta}$ can be estimated by minimizing the penalized least squares criterion:

$$\sum_i (Y_i - \mathbf{x}_i^T \boldsymbol{\phi})^2 + \lambda \sum_j |\phi_j|^\gamma \qquad \text{eqn. (2)}$$

OLS (ordinary least squares) estimation of linear regression estimates $\boldsymbol{\beta}$ by minimizing the residual sum of squares without the penalty term. However, OLS estimation is not satisfactory in an application like this with many predictors. One reason is that it has low prediction bias but large variance. The predictive accuracy can be improved by adding the second penalty term in (2), which can be tuned by various criteria. Another reason for using the LASSO is that the interpretation of OLS estimators can be difficult with a large number of predictors. "Unguided" OLS includes all of them in the model; this generally results in a model "over fitting" the observations at the expense of poor (out of sample) predictions. .

When $\gamma = 1$, which is the case of LASSO, the estimators minimizing (2) have the potential of being exactly 0 if λ is sufficiently large. Thus the LASSO algorithm effectively does both model selection and parameter estimation. The issue of model selection is particularly important in this case with comparatively few observations and many predictors.

We have several criteria on which to tune the parameter λ which penalizes models with many variables. We use Mallow's C_p, and the Bayesian Information Criterion (BIC).

Mallow's C_p is defined as $C_p = \frac{SSE_p}{S^2} - N + 2P$, in which SSE_p is the error sum of squares with p predictors, N is the sample size, and S^2 is the residual mean square regressed on the complete data. The term p is the number of predictors, so C_p penalizes overfitting.

Another criterion is the BIC. In regression cases, it is defined as $BIC = n\log(1-R^2) + p\log n$ where n is the number of observations and p the number of predictors. The BIC also represents a tradeoff between the fit and the complexity. When *log n>2,* the BIC has larger penalties for more variables, and tends to select fewer variables than with Mallow's Cp.

Best subsets regression

The best subsets method finds "best" subsets of predictors for models of varying sizes (numbers of predictors) based on r-squared, or equivalently, the least squares criterion. The models can be compared using Mallow's C_p and BIC, finding the best model according to either of the two criteria.

Results

Appendix Table D.4 shows the model selection result with the two methods: LASSO and best subsets. The LASSO, minimizing BIC, chose a model with 10 predictors. We can see from the right panel of Appendix Figure D.1 that the BIC value increases rapidly with the size of the model beyond 10 predictors. On the other hand, as shown in left panel, Mallow's C_p does not get notably worse when increasing the model size beyond 10 predictors. The sizes of the model

selected by BIC and the Mallow's C_p are not always the same. However in this case we obtain arguably 10 predictors chosen by the LASSO model with either the BIC or the Mallow's C_p criterion.

The Best subsets regression selects 11 predictors with the Mallow's C_p criterion, and 7 with BIC (Appendix Figure D.4). As shown in Appendix Table D.4, some of the predictors selected by best subsets are consistent with the ones selected by the LASSO, while others are not.

The difference in the two selected models comes from different methods of model selection. The major difference is that the LASSO penalizes large coefficients to find a balance between the bias and the variance, while best subsets regression does not. In this sense, C_p and BIC, despite being similarly calculated, are not directly comparable between the LASSO and best subsets models. As we will see shortly, given just the set of LASSO predictors the R-squared, C_p, and BIC could all be improved by fitting the coefficients with OLS rather than the penalized criterion. Thus, caution is advised in interpreting the best subsets models as predictively superior to the LASSO solely based on the disparity in R-squared, C_p, and BIC in Appendix Table D.4.

Candidate models with OLS

We now use traditional means by which to evaluate the selected variables. We will examine the OLS results for the variables selected by the LASSO as well as best subsets.

OLS results for LASSO predictors

Appendix Table D.6 shows the standardized coefficients for the variables selected by the LASSO using OLS along with the estimates from the LASSO itself. The DTT response is not

standardized. We notice that components Br, Ce, La, Se, and V do not appear individually significant at the 0.05 level, although they are included in the model selected by the LASSO; they contribute jointly to the quality of prediction. We note that none of these five variables appear in *both* the models selected by best subsets (Appendix Table D.4). The difference in the estimated coefficients between the LASSO fit and the OLS fit of LASSO-selected variables underscores the general coefficient shrinkage that occurs with the LASSO R-squared is naturally larger for the OLS fit (0.31) than for the LASSO fit (0.25), commensurate with minimizing in-sample squared error.

OLS results for best subsets predictors

Appendix Table D.7 shows the standardized coefficients for the 11 variables selected by best subsets with the C_p criterion used to select the best model. We see that nearly all the predictors are significant at a level of 0.05, with the one that is not, Zn_conc, very close to this threshold of evidence.

$PM_{2.5}$ and Location-Season effects

Phases two and three of the modeling strategy involve adding $PM_{2.5}$ and location-season effects in sequence to investigate the incremental benefit of these predictors. To do this, we proceed with the conventional approach of adding these predictors and assessing the significance by F-tests as well investigating the influence of these additions on other predictors.

There are two parallel models, the LASSO and best subsets predictors, with which to proceed. As the best subsets method is still more conventional, we proceed with this model as a baseline on which to assess $PM_{2.5}$ and location-season.

Phase 2: $PM_{2.5}$.

The addition of $PM_{2.5}$ to the baseline model is significant at a 0.05 level ($F_{1,232}$=5.38, p-value = 0.02). The results expressed in both unstandardized and standardized coefficients are shown in Appendix Table D.8. Note that as Group A and Group B predictors are composites, the choice of scale is arbitrary and thus duplicate values are not shown. All predictors are centered, meaning that the intercept reflects the fitted value when all predictors are set at their respective mean values.

With the inclusion of $PM_{2.5}$, the evidence for the inclusion of some of the predictors is weakened; specifically, predictors Cl, Zn, and Au are no longer statistically significant at a 0.05 level, although they remain close to being so.

Phase 3: Location and season effects

With 9 locations, 2 seasons, and the plausibility that seasonal effects differ by location, there are 18 different combinations of location and season resulting in an additional 17 parameters in the model. The addition of location-season main effects and interactions is significant at a 0.05 level ($F_{17,215}$=3.49, p-value < 0.001). The subsequent estimates for the existing predictors, expressed in both unstandardized and standardized coefficients, are shown in Appendix Table D.9.

With the inclusion of location-season effects, many predictors become insignificant. These include Cl, Zn, and Ti most severely, but also Se, Au, EC, and $PM_{2.5}$. Group B, Ag, OC, Group A, and Hf remain significant at a 0.05 level.

We may also examine the location-season specific intercepts for DTT reactivity, set at the global mean values for each of the predictors. These, along with the number of samples per location-season and standard errors appear in Appendix Table D.10.

Discussion

A few different approaches to variable selection were attempted. Based on tradeoffs between fit and model complexity, the following two models were pursued:

1. The LASSO, used for variable selection, selected the variables Ag, Br, Ce, Cl, La, Se, V, Zn, OC, and Group B. In an OLS fit with these same variables, Ag, Cl, Zn, OC, and Group B were significant at a 0.05 level. Group B represents the combination of S and P, of which S occurs at much higher concentrations.
2. Best subsets regression using C_p selected variables Ag, Au, Cl, Hf, Se, Ti, Zn, EC, OC, Group A, and Group B. Nearly all of these were significant at a 0.05 level, with Zn nearly so. Group A represents a combination of Ba, Cu, K, and Sr with K occurring at the highest concentrations of the four.

The LASSO is oriented towards prediction for which variable selection is a by-product. As such, it is inadvisable to discard the predictors from the LASSO as insignificant in an OLS treatment or discard LASSO results solely based on comparing in-sample measures such as R-squared, C_p, or BIC.

For formal inference about the significance of $PM_{2.5}$ and location-season effects, selected predictors from the best subsets (C_p) model were used as a baseline model to which these were added. $PM_{2.5}$ was found to be significant when added to the baseline model. Location and season effects were also found to be significant, implying that a significant amount of DTT reactivity cannot be explained solely based on $PM_{2.5}$ and identifiable components.

We summarize the fitted models in terms of conventional measures residual standard error, R-squared, and BIC in Appendix Table D.11. $PM_{2.5}$ explains significant variation in DTT unexplained by the component concentrations, while the city and season effects represent

sources of variability not represented by filter component measurements. Further, though conventional statistical tests indicate the significance of $PM_{2.5}$ and location-season effects, BIC, which penalizes more severely for model complexity, suggests that the baseline model is better, or at parity with, the more complex models. The models attempted are modestly predictive, with R-squared's ranging from 0.35 to 0.50.

Appendix Table D.1: Summary statistics for measurements of DTT reactivity

Total number of extracts analyzed (including duplicates)	365
number of extracts <LOQ	25 (6.8%)
Range of DTT reactivity values	0.16 – 8.53 μM/min
Mean (SD) DTT reactivity	3.31 (1.25) μM/min
Median DTT reactivity	3.28 μM/min
Precision (relative percent difference between duplicate filters)	11%

Appendix Table D.2: Summary of DTT Reactivity

	N	Mean	Std Dev	Min	Median	Max
DTT Reactivity (ng/min/m^3)	245	11.04	3.62	0.17	10.38	27.00

Appendix Table D.3: Summary of the predictors of DTT reactivity. Concentrations reported in units of ng/m3 for chemical species and

10^{-8}/m for LAC.

Predictor	Number less than Limit of Detection	Mean	Std Dev	Min	Median	Max	Correlation with DTT reactivity
Ag_conc	42	0.9	1.1	0.0	0.8	5.1	0.18
Al_conc	0	34.3	23.8	0.0	30.3	145.3	-0.07
As_conc	6	0.9	0.5	0.0	0.9	2.7	0.12
Au_conc	0	0.0	0.1	0.0	0.0	0.9	0.08
Ba_conc	12	10.2	13.5	0.6	6.4	112.4	-0.13
Br_conc	0	3.7	1.4	1.1	3.5	9.8	0.14
Ca_conc	0	75.5	41.0	16.8	68.3	213.2	-0.06
Cd_conc	85	1.2	1.2	0.0	0.9	5.5	-0.08
Ce_conc	21	0.6	0.6	0.0	0.4	2.5	-0.22
Cl_conc	0	7.8	46.5	0.0	0.0	536.2	0.18
Co_conc	28	0.1	0.3	0.0	0.0	2.1	0.04
Cr_conc	82	1.0	1.9	0.4	0.7	29.3	-0.04
Cs_conc	0	0.5	0.9	0.0	0.0	4.5	-0.04
Cu_conc	3	6.4	6.6	1.0	4.6	57.2	-0.08
Eu_conc	13	0.9	1.6	0.0	0.1	17.2	-0.03
Fe_conc	0	113.4	63.6	27.4	97.8	370.0	0.03
Ga_conc	23	0.3	0.5	0.0	0.2	5.4	0.02
Hf_conc	147	1.1	1.2	0.0	0.9	12.5	-0.11
Hg_conc	0	0.1	0.2	0.0	0.0	1.1	-0.06
In_conc	51	1.4	1.5	0.0	1.0	6.8	-0.05
Ir_conc	0	0.5	1.1	0.0	0.0	9.3	-0.09
K_conc	0	121.4	189.2	25.9	73.0	1,306.9	-0.11
La_conc	0	0.6	0.9	0.0	0.0	5.9	-0.16
LAC	0	7,443.3	3,945.7	1,966.0	6,662.0	23,120.0	0.08
Mg_conc	84	33.5	27.1	0.0	40.4	176.4	0.00
Mn_conc	0	3.3	2.0	0.4	2.8	13.9	0.10

Appendix Table D.3 (cont.): Summary of the predictors of DTT reactivity. Concentrations reported in units of ng/m^3

Predictor	Number less than Limit of Detection	Mean	Std Dev	Min	Median	Max	Correlation with DTT reactivity
Mo_conc	11	0.5	0.6	0.0	0.4	6.3	0.04
Na_conc	0	43.4	104.3	0.0	0.0	566.9	-0.21
Nb_conc	0	0.1	0.3	0.0	0.0	1.6	-0.04
Ni_conc	17	1.4	2.1	0.0	0.6	10.9	-0.16
P_conc	0	30.4	10.6	7.7	28.4	68.8	-0.15
Pb_conc	0	3.7	2.8	0.0	3.3	31.3	0.16
Rb_conc	161	0.5	0.2	0.2	0.5	1.5	-0.12
S_conc	0	1,429.4	622.0	386.2	1,324.1	3,230.6	-0.18
Sb_conc	111	5.6	3.9	0.0	4.8	27.3	0.10
Sc_conc	30	0.1	0.3	0.0	0.0	1.6	-0.09
Se_conc	0	1.1	0.6	0.0	0.9	3.3	0.18
Si_conc	0	120.6	52.8	39.7	112.3	351.5	-0.11
Sm_conc	0	0.1	0.3	0.0	0.0	4.0	-0.03
Sn_conc	171	6.5	2.3	3.4	6.2	15.1	0.02
Sr_conc	22	1.5	3.9	0.0	0.6	32.3	-0.15
Ta_conc	75	0.6	1.2	0.0	0.5	13.6	-0.01
Tb_conc	28	4.2	5.1	0.0	2.7	30.0	-0.06
Ti_conc	0	5.3	3.2	0.7	4.5	27.7	-0.09
V_conc	0	2.1	2.3	0.0	0.7	8.9	-0.31
W_conc	234	1.8	0.8	0.9	1.7	9.0	0.05
Y_conc	57	0.3	0.3	0.0	0.3	1.2	-0.12
Zn_conc	0	17.8	13.2	2.9	14.0	92.4	0.18
Zr_conc	43	0.9	0.8	0.0	0.7	5.2	0.02
EC_conc	1	1,445.1	654.6	0.3	1,280.0	4,610.0	0.12
OC_conc	22	2,008.0	751.6	811.3	1,900.0	4,970.0	0.27
PM2.5_conc	**0**	**13,985.2**	**4,498.1**	**5,356.7**	**13,550.2**	**31,576.3**	**0.04**

Appendix Table D.4. Selected predictors by the LASSO and the best subsets method.

	LASSO (Cp/BIC)	Best Subsets (Cp)	Best Subsets (BIC)
GroupB	X	X	X
Cl_conc	X	X	X
Ag_conc	X	X	
Se_conc	X	X	X
Zn_conc	X	X	X
OC_conc	X	X	X
La_conc	X		X
Br_conc	X		
Ce_conc	X		
V_conc	X		
Ti_conc		X	X
GroupA		X	
Au_conc		X	
Hf_conc		X	
EC_conc		X	
R-squared	0.25	0.35	0.30
Cp	26.2	-4.9	3.6
BIC	-9.5	-39.0	-43.0

Appendix Table D.5: Grouping of predictors of DTT reactivity determined by inspection of pairwise correlations.

Group 1 ("Group A"):

	Cu	K	Sr
Ba	0.95	0.92	0.93
Cu		0.83	0.86
K			0.96

Group 2

	Ca	Mn	Si
Al	0.53	0.35	0.73
Ca		0.66	0.65
Mn			0.40

Group 3

	lac	Ti	Zr	EC
Fe	0.88	0.75	0.72	0.75
Lac		0.65	0.72	0.81
Ti			0.51	0.54
Zr				0.55

Group 4

	V
Na	0.68

Group 5 ("Group B")

	S
P	0.80

Appendix Table D.6: LASSO and OLS estimates for the LASSO predictors

	LASSO Estimate	OLS Estimate	Std.Error	T value	Pr(>|t|)
(Intercept)		11.06	0.20		
V_conc	-0.48	-0.31	0.30	-1.04	0.301
OC_conc	0.71	1.18	0.25	4.62	<0.001
Ce_conc	-0.24	-0.35	0.23	-1.57	0.117
Cl_conc	0.26	0.51	0.20	2.55	0.011
Br_conc	0.25	0.39	0.25	1.53	0.127
Ag_conc	0.20	0.42	0.20	2.06	0.041
Zn_conc	0.22	0.54	0.21	2.58	0.010
GroupB	-0.45	-1.13	0.30	-3.72	<0.001
La_conc	-0.07	-0.27	0.22	-1.25	0.214
Se_conc	0.08	0.43	0.25	1.73	0.086
R-squared	0.25	0.31			

Appendix Table D.7: OLS estimates for the best subsets predictors

	Estimate	Std.Error	T value	Pr(>|t|)
(Intercept)	11.06	0.19	57.85	<0.001
GroupB	-1.48	0.25	-5.98	<0.001
Ag_conc	0.42	0.20	2.10	0.037
Cl_conc	0.56	0.19	2.87	0.005
Se_conc	0.74	0.23	3.17	0.002
Zn_conc	0.42	0.22	1.92	0.056
OC_conc	1.20	0.25	4.74	<0.001
GroupA	-0.50	0.21	-2.37	0.019
Au_conc	0.42	0.19	2.15	0.033
Hf_conc	-0.48	0.21	-2.33	0.021
Ti_conc	-0.72	0.24	-3.01	0.003
EC_conc	0.87	0.30	2.84	0.005
R-squared	0.35			

Appendix Table D.8: The baseline model for DTT reactivity with the addition of $PM_{2.5}$

	Unstandardized Estimate	Standardized Estimate	Std.Error	T value	Pr(>|t|)
(Intercept)	---	11.057	0.1894		
group B	---	-2.01	0.34	-6.00	<0.001
Ag_conc	363.18	0.41	0.20	2.08	0.039
Cl_conc	7.44	0.35	0.21	1.62	0.106
Se_conc	1257.39	0.75	0.23	3.25	0.001
Zn_conc	28.60	0.38	0.22	1.75	0.082
OC_conc	1.48	1.11	0.25	4.39	<0.001
group A	---	-0.58	0.21	-2.73	0.007
Au_conc	2759.55	0.35	0.19	1.83	0.069
Hf_conc	-355.92	-0.44	0.21	-2.13	0.034
Ti_conc	-268.91	-0.85	0.24	-3.49	<0.001
EC_conc	1.18	0.78	0.30	2.55	0.011
$PM_{2.5}$	0.18	0.82	0.35	2.32	0.021
R-squared	0.36				

Appendix Table D.9: The baseline+$PM_{2.5}$ model for DTT reactivity with the addition of location-season effects

	Unstandardized Estimate	Standardized Estimate	Std.Error	T value	Pr(>|t|)
group B	See Standardized	-1.04	0.45	-2.30	0.022
Ag_conc	334.34	0.38	0.19	1.99	0.047
Cl_conc	3.08	0.14	0.22	0.65	0.516
Se_conc	655.87	0.39	0.28	1.39	0.165
Zn_conc	15.39	0.20	0.27	0.76	0.448
OC_conc	1.61	1.21	0.31	3.89	<0.001
groupA	See Standardized	-0.45	0.20	-2.21	0.028
Au_conc	2768.88	0.36	0.20	1.77	0.078
Hf_conc	-382.64	-0.47	0.21	-2.22	0.027
Ti_conc	-59.29	-0.19	0.27	-0.69	0.488
EC_conc	0.93	0.61	0.36	1.67	0.097
PM2.5	0.13	0.58	0.43	1.36	0.175
R-squared	0.50				

Appendix Table D.10: Location-seasons intercepts for DTT reactivity.

Location	Season	N	Estimated Intercept (ng/min/m^3)	Std. Error
Baltimore	Summer	25	9.3	0.7
	Winter	19	12.1	0.7
Chicago	Summer	37	11.1	0.5
	Winter	16	13.2	0.9
Los Angeles	Summer	14	9.0	0.9
	Winter	3	11.5	1.7
Los Angeles-Coastal	Summer	23	10.6	0.7
	Winter	10	9.6	1.0
Los Angeles-Riverside	Summer	11	9.8	1.0
	Winter	1	6.9	3.2
New York	Summer	8	11.0	1.4
	Winter	6	10.3	1.4
New York-Rockdale	Summer	6	12.1	1.3
	Winter	2	10.6	2.0
St. Paul	Summer	21	10.7	0.7
	Winter	11	14.5	1.0
Winston-Salem	Summer	17	9.2	0.9
	Winter	15	15.0	0.9

Appendix Table D.11: Model comparisons for predicting DTT reactivity

Model	Number of Predictors	Residual Std Error	R-squared	BIC
Baseline (Best Subsets)	11	3.0	0.35	1291.5
Baseline + $PM_{2.5}$	12	3.0	0.36	1291.4
Baseline + $PM_{2.5}$ + Location-season	29	2.7	0.50	1325.2

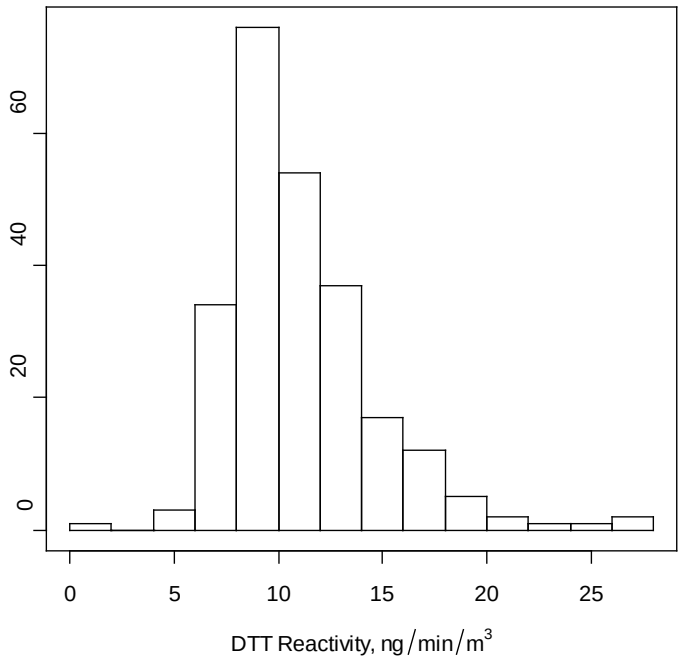

Appendix Figure D.1: Histogram of DTT Reactivity

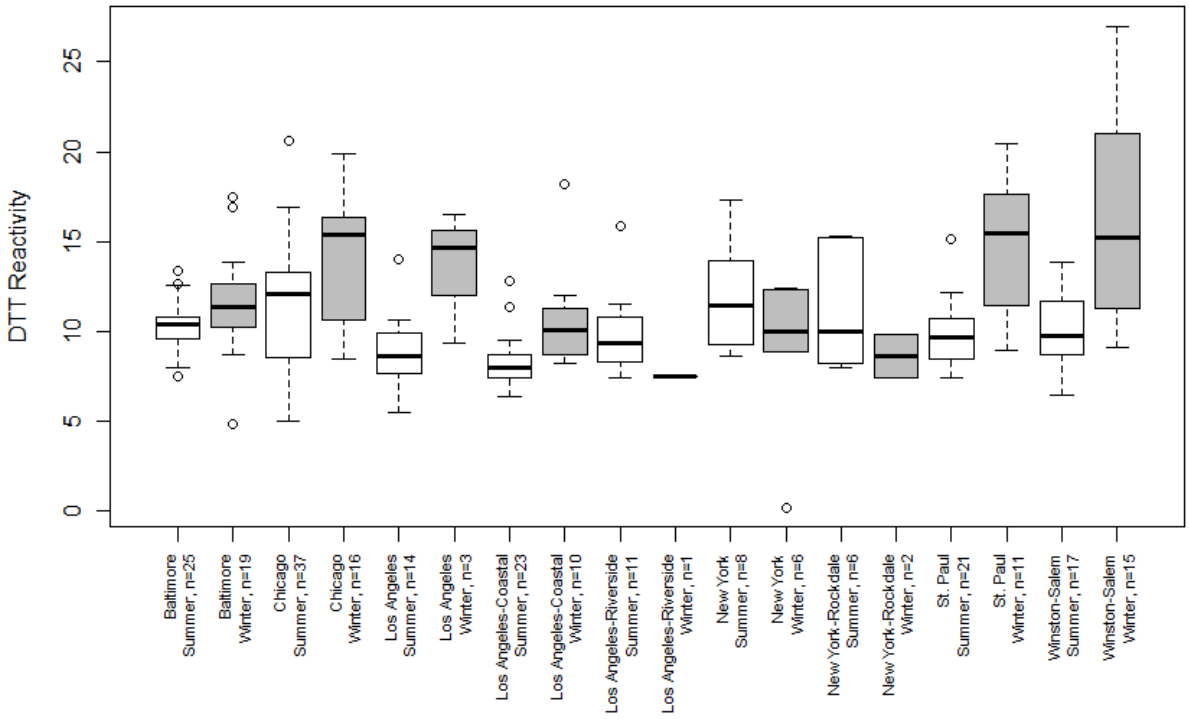

Appendix Figure D.2: DTT reactivity by location and season

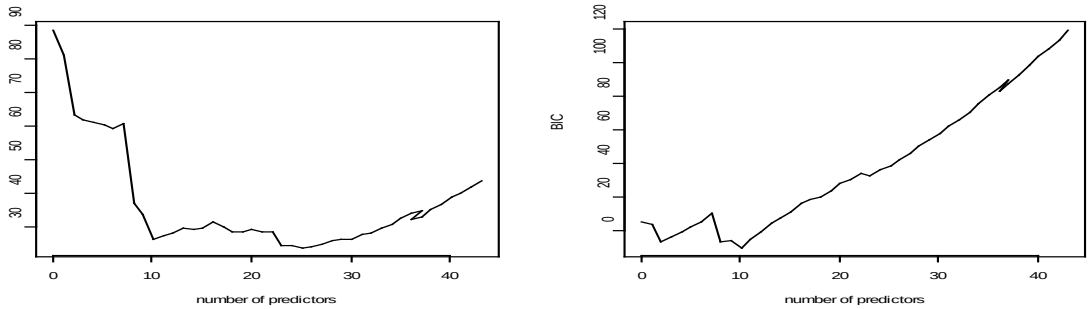

Appendix Figure D.3A The choice of predictors by the two criteria with the LASSO. (Left panel: Mallows Cp; right panel: BIC)

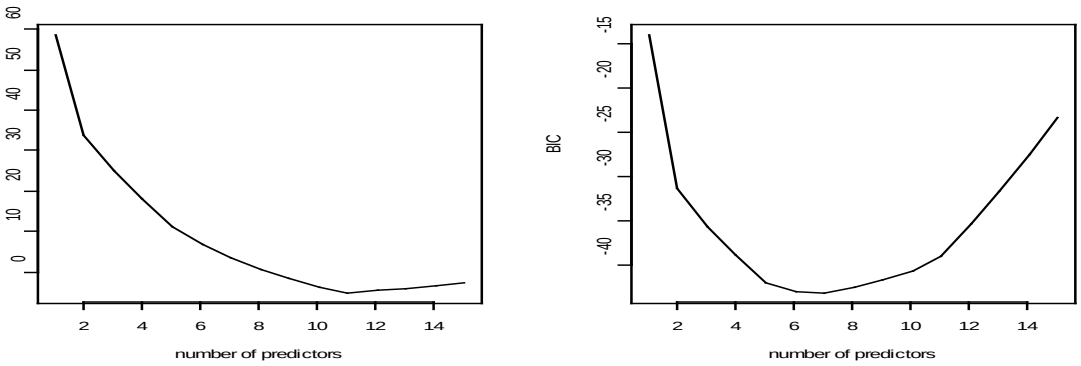

Figure D.4. The choice of predictors by the two criteria with best subsets method. (Left panel: Mallows Cp; right panel: BIC)

APPENDIX D.2: QC DATA FOR DTT MEASUREMENTS

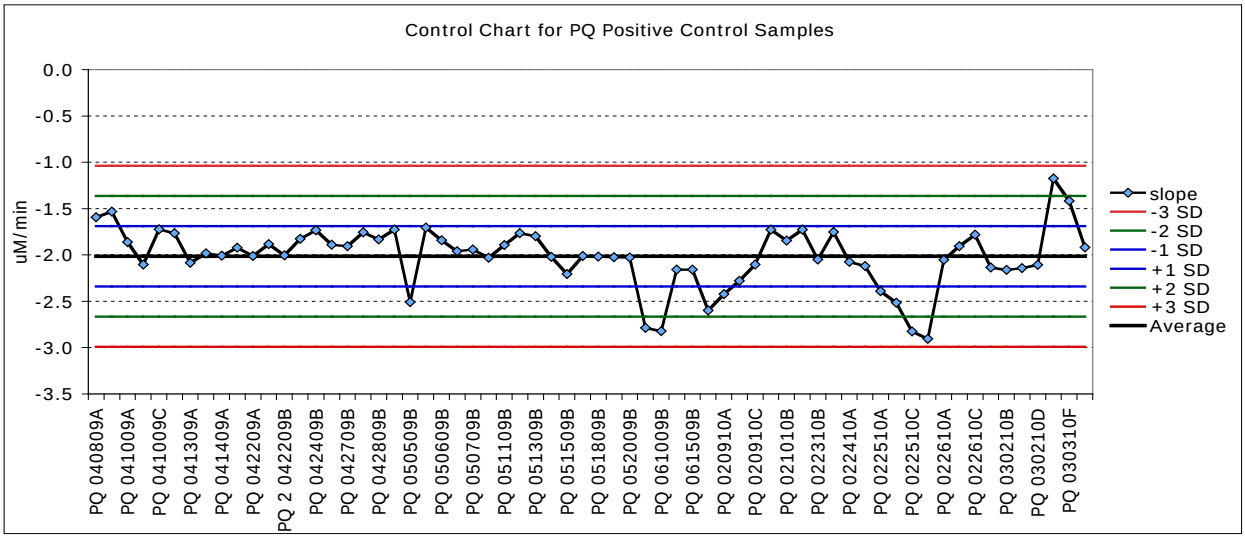

Appendix Figure D.2.1: Control chart illustrating variability in DTT oxidation response for phenathraquinone (PQ) samples used as positive control in the DTT assay.

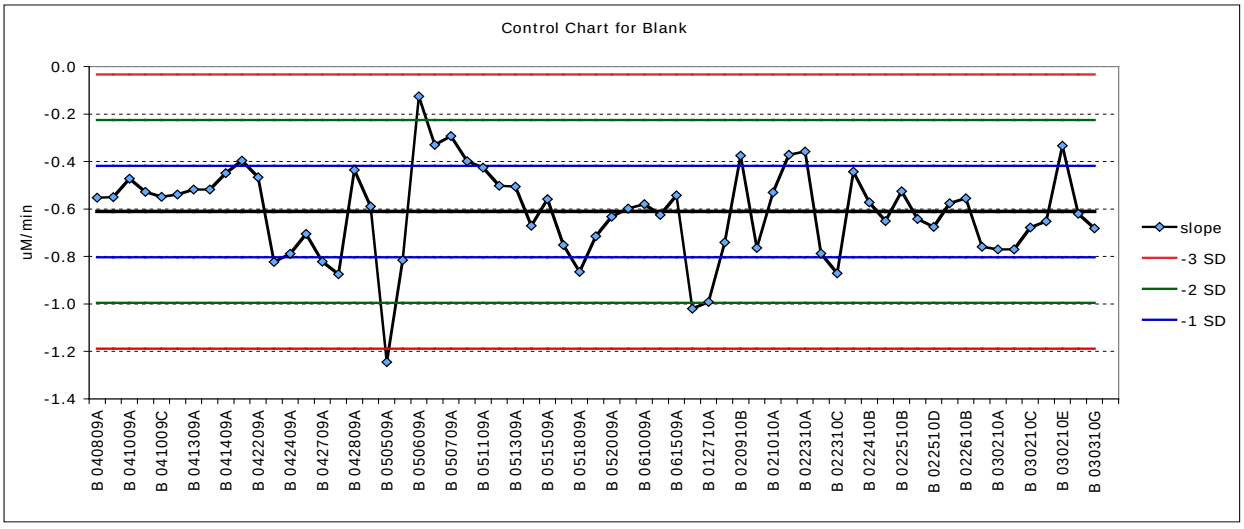

Appendix Figure D.2.2: Control chart illustrating variability in DTT oxidation response for extracts of blank filters in the DTT assay.

APPENDIX D.3: COMPARISON OF DTT REACTIVITY IN INTEGRATED PM SAMPLES WITH COLLECTION PERIODS OF 1-14 DAYS

An experiment was conducted to evaluate the stability of oxidative potential of particulate matter samples measured using the DTT assay. More specifically, the objective was to evaluate whether sampling with a single filter for an extended period of time would provide comparable results to the summation of values obtained from multiple filters collected contemporaneously over shorter durations, but having the same combined sampling time and volume of air.

Particulate matter samples were collected on pre-fired quartz filters in early summer, 2009, for analysis of oxidative potential. Filters were collocated on the rooftop of a University of Southern California building. Three, two-week sampling sessions were conducted (6/1/09-6/15/09, 6/15/09-6/29/09, and 6/29/09-7/13/09). For each session, a single two week sample was collected in parallel with four intermediate samples (3 or 4 days) covering the same time period. Additionally, with each session, seven daily filters were collected corresponding to two of the intermediate filters.

After sampling, filters were placed in individual plastic petri dishes with lids, wrapped in aluminum foil, sealed in ziplock bags and stored in a -20°C freezer for approximately six months prior to analysis for oxidative potential using the DTT assay.

Results

Appendix Table D.2.1 illustrates the relationship in time between the daily intermediate (3-4 day) and 2-week composite samples for each of the three sampling campaigns. One of the 3-day samples (sample id# QH-L-F-052-103-S) was excluded from the analysis because the pump failed after seven hours.

First event June 1 – June 15, 2009

Day	2-week composite	Intermediate	Daily
1	QH-L-F-051-001-S	QH-L-F-052-101-S	QH-L-F-053-111-S
2			QH-L-F-053-112-S
3			QH-L-F-053-113-S
4			QH-L-F-053-114-S
5		QH-L-F-052-102-S	Not collected
6			Not collected
7			Not collected
8			Not collected
9		QH-L-F-052-103-S	QH-L-F-053-131-S
19			QH-L-F-053-132-S
11			QH-L-F-053-133-S
12		QH-L-F-052-104-S	Not collected
13			Not collected
14			Not collected

Second event June 15 – June 29, 2009

Day	2-week composite	Intermediate	Daily
1	QH-L-F-051-002-S	QH-L-F-052-201-S	QH-L-F-053-211-S
2			QH-L-F-053-212-S
3			QH-L-F-053-213-S
4			QH-L-F-053-214-S
5		QH-L-F-052-202-S	Not collected
6			Not collected
7			Not collected
8			Not collected
9		QH-L-F-052-203-S	QH-L-F-053-231-S
19			QH-L-F-053-232-S
11			QH-L-F-053-233-S
12		QH-L-F-052-204-S	Not collected
13			Not collected
14			Not collected

Third event June 29 – July 13, 2009

Day	2-week composite	Intermediate	Daily
1	QH-L-F-051-003-S	QH-L-F-052-301-S	QH-L-F-053-311-S
2			QH-L-F-053-312-S
3			QH-L-F-053-313-S
4		QH-L-F-052-302-S	Not collected
5			Not collected
6			Not collected
7			Not collected
8		QH-L-F-052-303-S	QH-L-F-053-331-S
9			QH-L-F-053-332-S
19			QH-L-F-053-333-S
11			QH-L-F-053-334-S
12		QH-L-F-052-304-S	Not collected
13			Not collected
14			Not collected

Appendix Table D.3.1: Relationship between daily, intermediate and 2-week composite samples.

Appendix Figure D.3.1 illustrates the comparison between the 2-week composite samples and the corresponding time weighted average of the four intermediate (3 or 4 day) samples collected over the same period as the two week composites. Figure D.3.2 illustrates a similar comparison between the intermediate (3 or 4 day) samples and the corresponding daily samples.

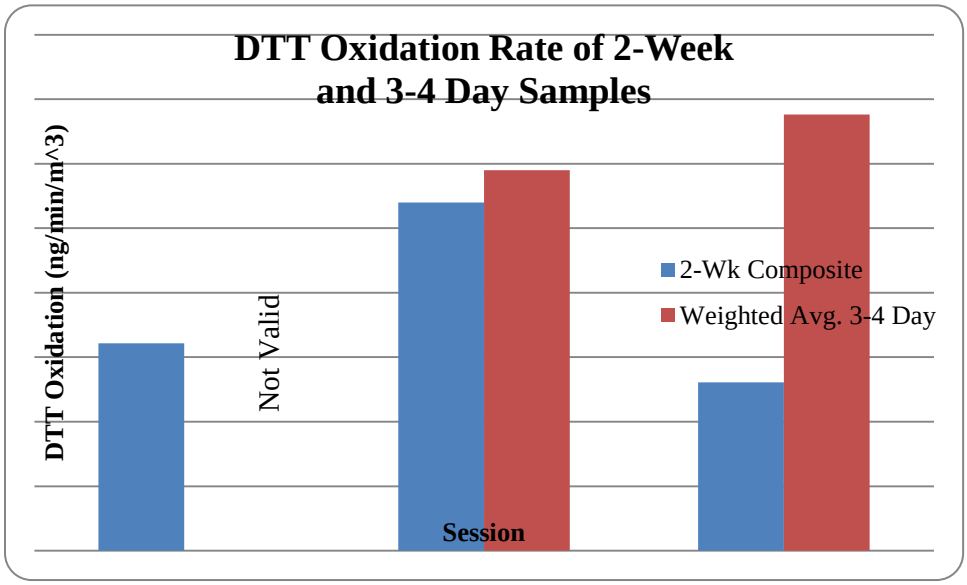

Appendix Figure D.3.1: Comparison between two week composite samples and the time weighted average of the four corresponding intermediate (3 or 4 day) samples.

In Appendix Figure D.3.2, measurements of DTT reactivity were in good agreement between the intermediate and long term samples for one of two paired samples. In Appendix Figure D.3.2, measurements of DTT reactivity were in good agreement between the intermediate and daily samples for three of five paired samples. In all cases the DTT reactivity determined as the average of the daily samples was greater than the DTT reactivity measured for the corresponding intermediate (2-4 day) sample.

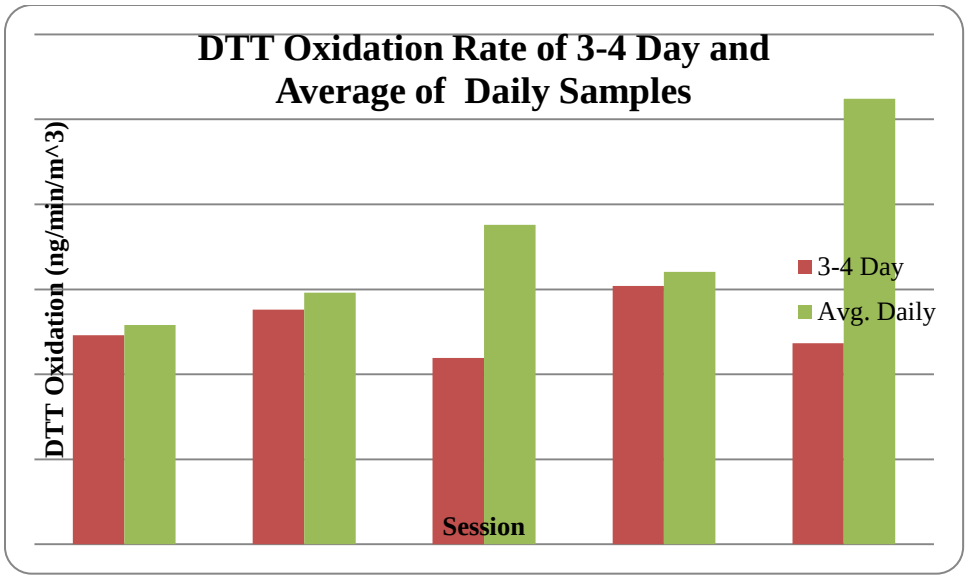

Appendix Figure D.3.2: Comparison between intermediate (3-4 day) samples and the average of the four corresponding daily samples.

The observation of lower reactivity in the intermediate samples compared to the daily samples raises the possibility that some of the reactive species in the PM samples become oxidized over time after collection on the filter, and having been so-oxidized are subsequently unable to oxidize DTT in the laboratory assay (i.e. DTT reactivity of the particles decays over time). However, the limited number of samples analyzed in the current study, and the fact that consistent, substantial differences in DTT reactivity between short term and longer term samples does not provide clear evidence of a loss of DTT reactivity as sampling time is increased.

Conclusions

Higher absolute DTT oxidation rates were observed from filters with longer sampling times (i.e. total DTT reactivity for 2-week samples was greater than 3-4 day samples, and daily samples were the least reactive). This is to be expected due to the greater air volume sampled

and particulate matter collected. When oxidation rates were normalized to sample volume, the shorter duration samples were more reactive, overall. However, good agreement was observed in three out of five sample sets comparing 1-day and 3-4 day periods. One of two valid sample sets showed good agreement between 3-4 day and 2-week periods.